QSAR & Combinatorial Science QCS

Application of a Receptor Pruning Methodology to the Enoyl-ACP Reductase from *Escherichia coli* (FabI)

Kerly F. M. Pasqualoto* and Márcia M. C. Ferreira

Laboratory for Theoretical and Applied Chemometrics, Department of Physical Chemistry, Institute of Chemistry, building H, room 219, The State University of Campinas – UNICAMP, Campinas, SP 13084-971, P.O.B. 6154, Brazil; E-mail: kerly@netpoint.com.br.

Keywords: diazaborines, enoyl-acp reductase, receptor pruning model, structure-based design

Received: October 26, 2005; Accepted: January 3, 2006

DOI: 10.1002/qsar.200530182

Abstract

Receptor pruning is an approach for achieving reasonable conformational ensemble profile in terms of time and computational resources. The purpose of this study is to reduce the size of a model structure of enoyl-acp reductase (ENR) from *E. coli*, FabI, to allow ligand-receptor molecular dynamic (MD) simulations to be computationally economical yet still provide meaningful binding thermodynamic data. Three reduced-size models of FabI were created by pruning away all residues greater than 12, 10 and 8 Å radius. The largest ligand was docked in the active site to define the largest required receptor model. Energy minimization and MD simulations were carried out using the MOLSIM 3.2 program. The lowest energy structure for each of receptor models from MD calculation was compared by root mean square (RMS) fit to the equivalent portion of the crystal structure of FabI. A scale-down 12 Å receptor model of the enzyme FabI maintains the structural integrity of the composite parent crystal structure. The perspectives include the structure-based design of new antituberculosis agents regarding the similarity in the active site of two ENRs, FabI and InhA (*M. tuberculosis*).

1 Introduction

Diazaborines represent a group of antibacterial agents of which the important structural element is a heterocyclic 1,2-diazine ring containing a boron as a third hetero atom. The more systematic name for these compounds is 1,2-dihydro-1-hydroxy-2-(organosulfonyl)-areno[*d*][1,2,3]diazaborines. The arene group can be benzene, naphthalene, thiophene, furan and pyrrole [1–3] (Figure 1). Grassberger and co-workers [1] first described the syntheses of these compounds by the reaction of (organosulfonyl)hydrazones of arene aldehydes or ketones with tribromoborane in the presence of ferric chloride. They also determined the biological activities (*in vitro* and *in vivo*) of approximately 80 different diazaborine derivatives, and some structure-activity relationships were discussed. In general, thieno-diazaborines were found to be most potent inhibitors, followed by benzo-diazaborines and furo-diazaborines, whereas pyrrolo-diazaborines were totally inactive. The antibacterial activity of diazaborines is confined almost exclusively to Gram-negative bacteria, and initially, this was thought to be due to the prevention of lipopolysaccharide (LPS) synthesis, which is an integral part of the outer membrane of that group of bacteria [1].

More recently, the molecular target of diazaborines was identified as the enoyl-acp reductase (ENR), which is a component of the bacterial fatty acid synthase (FAS II) [1, 2]. ENR catalyzes the last reductive step in the cyclic process of fatty acid elongation, and it is considered the key enzyme of the FAS II pathway [2–6]. Studies have shown that the presence of the cofactor nicotinamide adenine dinucleotide (NAD) is required for both the inhibition and the binding of diazaborine to the ENR enzyme [7].

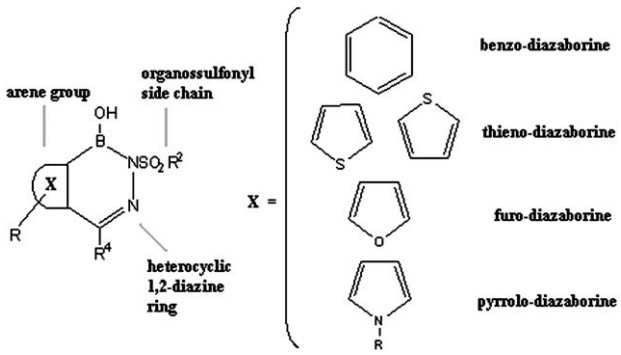

Figure 1. Structural formulae of different classes of diazaborines.

The best characterized FAS-II system is that of *Escherichia coli*, which includes β-ketoacyl-ACP synthases (FabB, FabF, and FabH), a β-ketoacyl-ACP reductase (FabG), β-hydroxyacyl-ACP dehydrases (FabA and FabZ), and an enoyl-ACP reductase (currently known as FabI and formerly known as EnvM) [4, 6, 8]. Enzymes that form the biosynthetic apparatus for fatty acid production are considered ideal targets for designing new antibacterial agents. The difference between the molecular organization of FAS found in most bacteria and mammals is the reason for this assumption [8–12].

The x-ray crystallographic structures of *E. coli* ENR, FabI, with bound NAD cofactor, and in complex with bound NAD and thieno-diazaborine or benzo-diazaborine were determined by Baldock and co-workers [2] at 2.09 Å, 2.2 Å, and 2.5 Å resolution, respectively. The analysis of the X-ray crystallographic structures of complexes of FabI with NAD and either thieno-diazaborine or benzo-diazaborine revealed the formation of a covalent bond between the 2' hydroxyl of the nicotinamide ribose and a boron atom in the ligands to generate a tight, noncovalently bound bisubstrate analogue. Besides of the implications for the structure based-design of inhibitors of ENR, this suggests that the utilization of the ribose hydroxyl to create a bisubstrate analogue might find important applications in other areas of medicinal chemistry, regarding the similarities in catalytic chemistry and in the conformation of the nucleotide cofactor to other oxidoreductases [2, 3].

Structure-based design (SBD) is the application of ligand-receptor modeling to predict the activity of a set of molecules that bind to a common receptor for which the molecular geometry is available. Successful SBD requires an accurate receptor model which can be economically employed in the design calculations. In other words, the computer-assisted molecular design (CAMD) tools necessary to extract information from a 3D receptor structure are computationally more economical when applied to smaller systems [13].

4D-QSAR analysis [14] has been used to develop 3D pharmacophore models because of its capability of exploring large degrees of both conformational and alignment freedoms in the search for the active conformation and binding mode, respectively, of each compound investigated. The receptor-dependent (*RD*) 4D-QSAR approach can be considered a method for performing quantitative structure-based design by extending the current receptor-independent (*RI*) 4D-QSAR [12, 15–18] methodology to include receptor geometry. Consequently, *RD* 4D-QSAR is, in fact, a structure based QSAR approach.

The *RD* 4D-QSAR formalism can previously employ a receptor-pruning technique, particularly when a reasonable ensemble profile must be achieved in terms of time and computational resources. Basically, pruning is considered a preprocessing operation to scale down the protein to a manageable size structure containing the lining of the binding site before undertaking the actual 4D-QSAR formalism [19, 20].

The purpose of this study is to reduce the size of a model structure of the macromolecular receptor, FabI ENR, by using the receptor pruning approach to allow multiple ligand-receptor molecular dynamic (MD) simulations to be computationally economical without essentials losses of meaningful binding thermodynamic data. The pruning technique employed here was based on that reported by Tokarski and Hopfinger [13].

In our next study, the scale-down receptor model will be considered for the application of a *RD* 4D-QSAR methodology to a set of 51 diazaborine derivatives (Tables 1–3).

Table 1. Structures and biological activities of the 2-(Organosulfonyl)-1,2,dihydro-1-hydroxy-2,3,1-benzodiazaborines **BD** [a]

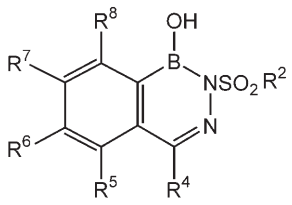

BD

BD	R^2	R^4	R^5	R^6	R^7	R^8	pMIC
40	*n*-C_3H_7	H	H	CH_3	H	H	5.17
32	4-$H_2NC_6H_4$	H	H	CH_3	H	H	5.19
37	4-$O_2NC_6H_4$	H	H	Br	H	H	5.23
1	4-$CH_3C_6H_4$	H	H	H	H	H	4.56
39	CH_3	H	H	CH_3	H	H	4.56
7	4-$CH_3C_6H_4$	H	H	F	H	H	4.59
30	4-$H_2NC_6H_4$	H	F	H	H	H	4.59
10	4-$CH_3C_6H_4$	H	H	Cl	H	H	4.60
15	4-$CH_3C_6H_4$	H	H	Br	H	H	4.62
34	2-Cl-4-$CH_3CONHC_6H_3$	H	H	CH_3	H	H	4.63
4	4-$CH_3C_6H_4$	H	H	CH_3	H	H	4.89
41	*n*-C_3H_7	H	H	Cl	H	H	4.98
33	2-Cl-4-$H_2NC_6H_3$	H	H	CH_3	H	H	5.01
31	4-$H_2NC_6H_3$	H	H	Br	H	H	5.02
5	4-$CH_3C_6H_4$	H	CH_3	H	H	CH_3	3.22
17	4-$CH_3C_6H_4$	H	H	H	OH	H	3.51
8	4-$CH_3C_6H_4$	H	H	H	F	H	3.59
2	4-$CH_3C_6H_4$	CH_3	H	H	H	H	3.99
9	4-$CH_3C_6H_4$	H	Cl	H	H	H	4.00
20	4-$CH_3C_6H_4$	H	H	$N(CH_3)_2$	H	H	4.00
36	4-$O_2NC_6H_4$	H	F	H	H	H	4.01
42	$(CH_3)_2N$	H	H	H	H	H	4.21
26	C_6H_5	H	H	H	OH	H	4.29
16	4-$CH_3C_6H_4$	H	H	H	Br	H	4.32
35	2-Cl-4-$CH_3CONHC_6H_3$	H	H	Br	H	H	4.35

[a] Activity was measured as the minimum inhibitory concentration (MIC) against strains of *E. coli* Δ120 at 310 K and given as pMIC (see ref 1).

Table 2. Structures and biological activities of the 2-(Organosulfonyl)-1,2,dihydro-1-hydroxythieno-[3,2-*d*][1,2,3]diazaborines **TD-b**, and the 2-(Organosulfonyl)-1,2,dihydro-1-hydroxythieno-[2,3-*d*][1,2,3]diazaborine **TD-c** [a]

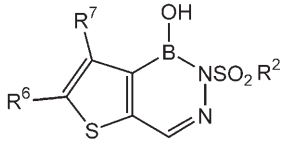

TD-b

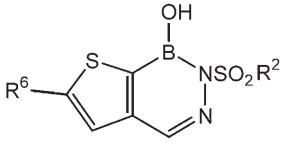

TD-

TD-b	R^2	R^6	R^7	pMIC	**TD-c**	R^2	R^6	pMIC
17b	*n*-C_3H_7	H	H	5.17	8c	$(CH_3)_2CHCH_2$	CH_3	5.18
1b	4-$CH_3C_6H_4$	Br	H	5.22	2c	4-$CH_3C_6H_4$	C_2H_5	5.20
8b	2-ClC_6H_4	C_2H_5	H	5.51	7c	*n*-C_3H_7	C_2H_5	5.58
3b	C_6H_5	Br	H	5.52	6c	*n*-C_3H_7	CH_3	5.87
18b	*n*-C_3H_7	CH_3	H	5.78	4c	2-ClC_6H_4	C_2H_5	5.01
5b	2-$CH_3C_6H_4$	CH_3	H	4.59	5c	2-Cl-4-$CH_3C_6H_3$	CH_3	4.31
11b	4-$CH_3C_6H_4$	Cl	H	4.60				
4b	2-$CH_3C_6H_4$	Br	H	4.62				
6b	2-ClC_6H_4	Br	H	4.63				
13b	4-$CH_3CONHC_6H_4$	Br	H	4.64				
7b	2-ClC_6H_4	CH_3	H	4.90				
19b	$(CH_3)_2CHCH_2$	Br	H	4.91				
12b	2,4,6-$(CH_3)_3C_6H_2$	Br	H	3.25				
15b	CH_3	H	H	3.90				
10b	2-Cl-4-$CH_3C_6H_3$	CH_3	H	4.31				
9b	2-Cl-4-$CH_3C_6H_3$	Br	H	4.34				
14b	2-Cl-4-$CH_3CONHC_6H_3$	Br	H	4.35				

[a] Activity was measured as the minimum inhibitory concentration (MIC) against strains of *E. coli* Δ120 at 310 K and given as pMIC (see ref 1).

Table 3. Structures and biological activities of the 2-(Organosulfonyl)-1,2,dihydro-1-hydroxyfuro-[3,2-*d*][1,2,3]diazaborines **FD**, and 2-(Organosulfonyl)-1,2,dihydro-1-hydroxypyrrolo-[3,2-*d*][1,2,3]diazaborine **PD** [a]

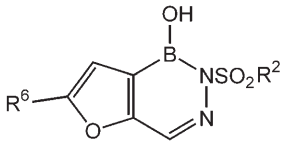

FD

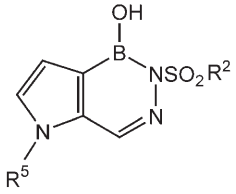

PD

FD	R^2	R^6	pMIC	**PD**	R^2	R^5	pMIC
1	4-$CH_3C_6H_4$	CH_3	4.89	3	4-$CH_3C_6H_4$	$C_6H_5CH_2$	3.24
2	4-$CH_3C_6H_4$	Br	4.92				

[a] Activity was measured as the minimum inhibitory concentration (MIC) against strains of *E. coli* Δ120 at 310 K and given as pMIC (see ref 1).

2 Methods

2.1 Generation of 3D structures

Baldock *et al.* co-crystallized a thieno- and a benzo-diazaborine bound to the cofactor NAD in the active site of *E. coli* ENR, FabI, at 2.2 Å and 2.5 Å of resolution, respectively [2]. The coordinates of these complexes were deposited in the Brookhaven Protein Databank (PDB) [21] under the entry codes 1DFH and 1DFG, respectively. The thieno-diazaborine bound to NAD (1DFH) corresponds to the compound TD-18b in Table 2, and the benzo-diazaborine corresponds to the compound BD-1 in Table 1.

It is known that the geometry of the enzyme with a bound ligand is more appropriate target for docking the potential inhibitors than attempting to start with the crystal structure of the unbound enzyme. Furthermore, the co-crystallized ligands in the complexes 1DFH and 1DFG have similar structural features to the set of diazaborine analogues under investigation.

The X-ray structure of FabI selected as a starting model for the receptor geometry was the 1DFH, which presents 2.2 Å of resolution. This structure has two polypeptide chains or subunits, but just one subunit was used to build the receptor model. The N-terminus and C-terminus were both modeled as neutral and CH_3 groups were used as the block groups. AMBER [22] partial charges were assigned to all atoms of the enzyme structure, except to the block groups, using the HyperChem 6.03 program [23]. The charge state of ionizable residues was modeled at neutral pH. Thus, Arg and Lys residues were assigned a 1.0 charge, and Glu and Asp were each assigned a −1.0 charge. Lone pair electrons were not modeled explicitly. The crystal structure of the FabI complex had no water molecules. The total charge of the enzyme is practically zero, which means that the protein is effectively neutral. The MOLSIM 3.2 program [24] was used to perform the energy min-

imization and MD calculations of the receptor model. The minimized structure of the receptor model was used as initial structure in receptor pruning procedure (item *2.2*).

A set of 51 diazaborine derivatives were selected from ref 1. Biological activities were evaluated as the minimum inhibitory concentration, MIC (μg/mL), against strains of *E.coli* Δ120 at 310 K. The minimum inhibitory concentrations of these compounds were converted to molar units and then expressed in negative logarithmic units, pMIC (-log MIC). The pMIC values are given in Tables 1 – 3 and comprise the set of dependent variables that will be used to perform the 4D-QSAR analysis [12,14 – 20]. The range of activity for the analogues is in about 4 (3.22 – 5.87) pMIC units. The set of 51 diazaborine analogues comprises 12 active compounds [BD-40, TD-17b, TD-8c, BD-32, TD-2c, TD-1b, BD-37, TD-8b, TD-3b, TD-7c, TD-18b, TD-6c], 21 compounds with medium activity [BD-1, BD-39, BD-7, BD-30, TD-5b, BD-10, TD-11b, BD-15, TD-4b, BD-34, TD-6b, TD-13b, FD-1, BD-4, TD-7b, TD-19b, FD-2, BD-41, BD-33, TD-4c, BD-31], and 18 inactive compounds [BD-5, PD-3, TD-12b, BD-17, BD-8, TD-15b, BD-2, BD-9, BD-20, BD-36, BD-42, BD-26, TD-10b, TD-5c, BD-16, TD-9b, BD-35, TD-14b].

It was presumed that all compounds would act forming an adduct with cofactor NAD in the active site of FabI. The adduct presents a covalent bond between the 2' hydroxyl of the nicotinamide ribose and a boron atom in the diazaborine derivatives to generate a tight, noncovalently bound bisubstrate analogue, as reported by Baldock and co-workers [2, 3].

The three-dimensional structures of each of the 51 analogues (Tables 1 – 3) in their neutral forms were constructed using the HyperChem 6.03 software. The crystallized structure of the thieno-diazaborine/NAD adduct in the active site of FabI (1DFH) was used as a reference geometry in the building up of those ligands containing a five-membered ring as the arene group. The benzo-diazaborine analogues were constructed using the crystallized structure of the benzo-diazaborine/NAD adduct (1DFG) as a starting geometry. Each structure was energy-minimized using the HyperChem 6.03 MM+ force field without any restriction. Partial atomic charges were computed using the AM1 [25] semiempirical method, also implemented in the HyperChem program.

The volume of all ligands was calculated using the grid method described by Bodor and co-workers [26] with the atomic radii of Gavezzotti [27]. The bounding surface was specified as van der Waals and the density of grid points was set as 50 points on cube side to carry out the volume calculations (HyperChem 6.03).

2.2 Determination of the effective size of a receptor model – Receptor pruning

The entire model of the FabI bound to NAD with thieno-diazaborine complex consists of 3923 atoms including hydrogens. The total number of atoms of each complex FabI-NAD-diazaborine analogue makes multiple ligand-receptor MD simulations computationally uneconomical. However, the sampling of ligand-receptor geometries is needed to gain a meaningful thermodynamic averaged ensemble profile of such a system which is a major component to the "fourth" dimension in the 4D-QSAR paradigm. Thus, modeling approximations were applied to scale down the FabI structure to a more manageable size. The analysis was restricted to those amino acid residues of the enzyme near the active-site region, considering that the ligand-receptor interactions are relatively short range as compared to the size of whole receptor. As already mentioned, pruning is a preprocessing operation before undertaking the real *RD* 4D-QSAR analysis.

Receptor pruning was performed using HyperChem 6.03. Boron atom of the bound thieno-diazaborine inhibitor was chosen as the center of the pruning volume (Figure 2). Three different reduced-size receptor models of FabI were modeled to examine how the size of the FabI structure could be reduced without loosing information regarding the binding process. These models were created by pruning away all residues greater than 12, 10, and 8 Å, respectively, from the center. If any one non-hydrogen atom of a residue was within the spherical cutoff, then that entire residue was included in the model. The pruning operation results in a receptor model that is comprised of a number of unconnected peptide fragments. To retain the integrity of the local geometric environment of the receptor, fragments separated by less than or equal to four intervening residues were connected by the missing residues of the original FabI sequence. Zero partial charge CH_3 block groups were used to complete the open ends of the peptide fragments of the pruned model. All atoms of the pruned receptor model, except the block groups, were assigned AMBER partial charges [22]. The atom charge assignment procedure was already described (item *2.1*). It was found necessary to apply a constraint to the backbone atoms of each peptide fragment in the pruned receptor models to "fix" their positions in space during all energy minimization and MD calculations. The backbone atoms were each assigned a fictitious mass of 5000 a.m.u. to prevent significant departures from the model geometries due to the exclusion of the rest of enzyme.

The cofactor NAD is also retained in the active site of the pruned receptor model. The set of diazaborine analogues investigated presents structures containing two different ring sizes for the arene group: a five-membered ring (thiophene, furan and pyrrole) and a six-membered ring (benzene). The largest inhibitor (adduct) from each arene size group of the set of diazaborine derivatives was docked in the active site in order to define the largest required receptor model. PD-3 and BD-35 were select as the largest representative ligands containing a five- and six-membered ring as the arene group, respectively (see Table 5).

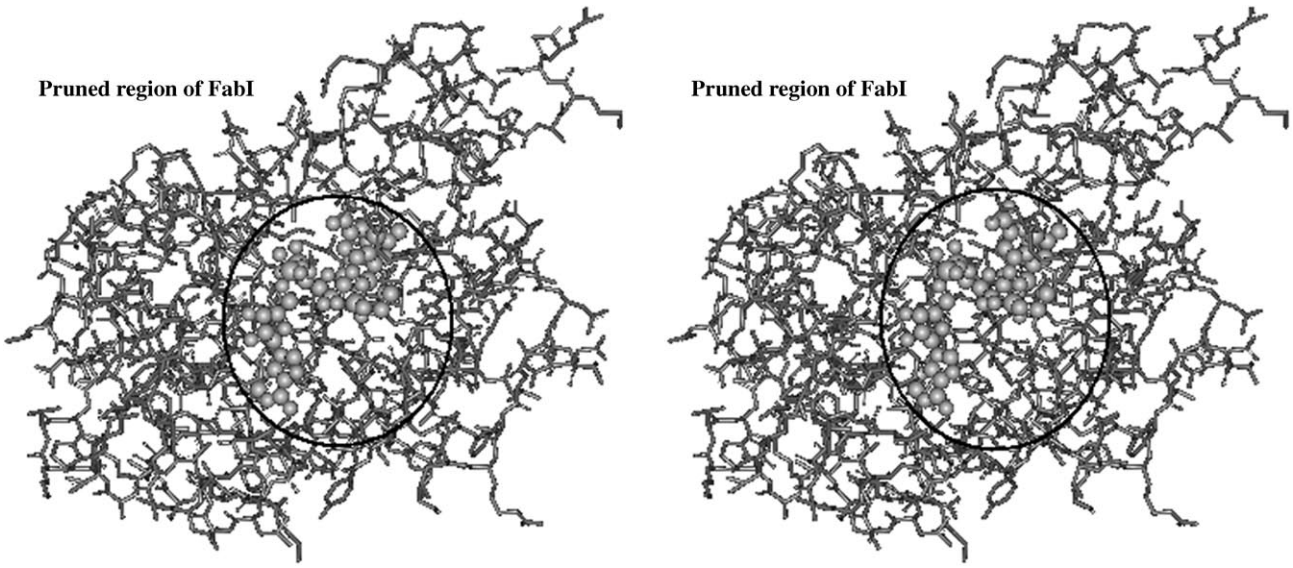

Figure 2. Stereoview of the thieno-diazaborine, TD-18b, and NAD bound to FabI. The protein structure is presented as stick model, and hydrogen atoms are hidden. The pruned receptor model of the protein is defined by the structure within the black circle. The ligand (thieno-diazaborine/NAD) is presented in CPK style, without hydrogens.

Conformation and alignment information for docking the largest ligand was based upon the bound structure of thieno-diazoborine (TD-18b), which was co-crystallized with FabI bound to NAD. The heterocyclic 1,2-diazine ring containing a boron atom is a common motif to all investigated ligands and its atomic coordinates in TD-18b was used to dock the largest ligands, PD-3 and BD-35.

As reported by Tokarski and Hopfinger [13], the evaluation of the stability of the different size receptor models was carried out by comparison of a representative structure of the scaled-down models obtained from a MD simulation (MDS) with that of crystallographically-determined structure.

Energy minimization and MD procedures were performed using the MOLSIM [24] program, version 3.2. The hydration shell model proposed by Hopfinger [28] was included in the force field representation to estimate aqueous solvation energies. Solvation energy contributions were only evaluated for the lowest energy structures. The molecular dielectric constant was set to a value of 3.5. The simulation temperature was 310 K, the same used in the biological assay [1].

The minimized structure of each of the pruned receptor models were used as the initial structures in each MD calculation. A MDS of 1ps at 310 K was performed on each of the scaled-down models using a nonbonded cutoff corresponding to the size of the model and a time step of 0.5 fs. In addition, a MDS 1ps at 310 K was carried out on the minimized structure of the entire receptor model employing each of the following nonbonded cutoffs: 12, 10 and 8 Å. The lowest energy structure for each of the receptor models from the MD simulations was compared by root mean square (RMS) fit to the equivalent portion of the entire receptor model, FabI, using HyperChem 6.03. In this study, the receptor pruned models presenting RMS fit values <1.5 Å to the whole enzyme FabI were considered acceptable, indicating no significantly structural deviation.

The ligand-receptor energy was examined for each of the scale-down receptor models using a nonbonded cutoff value of 12 Å. The cutoff of 12 Å was chosen to ensure that all possible interactions up to and including the distance of the largest receptor model size were being considered.

3 Results

The reduced receptor model of FabI with 8 Å radii is composed of 572 atoms from 28 amino acid residues and the diazaborine/NAD adduct. The 10 and 12 Å reduced-size receptor models present 875 and 1365 atoms, respectively, from 49 and 81 amino acid residues plus the adduct. The three pruned receptor models behave similarly with respect to RMS fit of all non-hydrogen atoms to the crystal structure over the course of the trial MD simulations. The RMS fit of the lowest energy structure of 8, 10 and 12 Å receptor models found in the MD procedures is 1.38, 1.06, and 1.08 Å, respectively, compared to the equivalent part of the lowest energy structure of entire FabI, as presented in Table 4. The RMS deviation of the whole enzyme structure from the MDS with respect to the crystal geometry is 1.20 Å.

The total energy of the lowest energy structure from MDS include the following energy contributions: bond stretching energy, bond angle bending energy, dihedral torsional energy, 1–4 interaction energy (Lennard-Jones),

Table 4. Total energy (E_{TOTAL}) and RMS deviation values found for the receptor pruned models with the co-crystallized ligand, TD-18b.

Receptor pruned models with the ligand TD-18b	E_{TOTAL}[a] (kcal/mol)	RMS fit[b] (Å)
8 Å radii	−2553.62	1.38
10 Å radii	−6211.67	1.06
12 Å radii	−16516.04	1.08

[a] Total energy, including solvation energy. [b] RMS deviation of receptor pruned compare to the entire FabI.

van der Waals interaction energy, electrostatics interactions energy, hydrogen bonding energy and solvation energy. The values of total energy obtained for the lowest energy structure of the 8, 10 and 12 Å receptor models are −2553.62, −6211.67 and −16516.04 kcal/mol, respectively (see Table 4). These values indicate that the pruned receptor model of 12 Å radii is more energetically stable.

The calculated volume of all ligands (diazaborine/NAD adducts) is shown in Table 5. The largest diazaborine analogue representative of the arene size group containing a five-membered ring is PD-3, a pyrrolo-diazaborine. The benzo-diazaborine BD-35 is the largest ligand having a six-membered ring as the arene group. These two ligands were docked in the active site of the lowest energy structure of 8, 10 and 12 Å receptor models using the atomic coordinates of the co-crystallized ligand TD-18b as reference.

The pruned receptor models of 8 Å radii containing the largest ligands PD-3 and BD-35 in the active site behave differently with respect to RMS fit of all non-hydrogen atoms to the entire enzyme over the course of the trial MD calculations. The RMS fit of the lowest energy structure of 8, 10 and 12 Å receptor containing the ligand PD-3 is 1.94, 1.13 and 1.27 Å, respectively. The RMS fit found for the lowest energy structure of 8, 10 and 12 Å receptor containing the ligand BD-35 is 2.40, 1.09 and 1.18 Å, respectively (see Table 6). According to those RMS deviation values, for both ligands (PD-3 and BD-35), the scaled-down receptor model of 8 Å radii did not maintain the structural integrity of the composite parent crystal structure.

The total energy (E_{TOTAL}) of the lowest energy structure of 8, 10 and 12 Å receptor containing the largest ligands PD-3 and BD-35, including solvation energy, are listed in Table 6. As can be seen, for the both ligands the 12 Å reduced-size receptor models present the more favorable total energy values.

The intermolecular ligand-receptor interaction energy, shown in Table 7, is the summation of the van der Waals, electrostatic, and hydrogen bonding energies. The RMS deviation values found for the lowest energy structures from MD simulations of the receptor pruned models and the entire FabI model, in terms of the backbone atoms, are also listed in Table 7. The lowest energy complex state sampled during the MD procedures was used to represent the receptor structure. The lowest energy complex of FabI with PD-3/NAD adduct bound presented the following energy contributions: total energy (E_{TOTAL}) of 2050.67 kcal/mol, ligand-receptor intermolecular interaction energy (E_{inter}) of −62541.30 kcal/mol, intramolecular energy of bound ligand (E_L) of −166.51 kcal/mol and intramolecular

Table 5. The calculated volume of all ligands.

Ligands (diazaborines + NAD = adducts)	Volume (Å^3)	
TD-6c	697.24	
TD-18b	697.11	
TD-7c	714.13	A
TD-3b	725.10	C
TD-8b	751.54	T
BD-37	756.08	I
TD-1b	741.96	V
TD-2c	754.18	E
BD-32	743.55	S
TD-8c	714.26	
TD-17b	680.17	
BD-40	710.21	
BD-31	748.38	
TD-4c	751.70	
BD-33	757.56	M
BD-41	707.80	E
FD-2	734.03	E
TD-19b	718.57	I
TD-7b	734.69	U
BD-4	749.86	M
FD-1	729.29	
TD-13b	770.92	
TD-6b	739.35	
BD-34	792.96	A
TD-4b	741.24	C
BD-15	754.69	T
TD-11b	734.82	I
BD-10	747.42	V
TD-5b	736.63	I
BD-30	729.03	T
BD-7	735.30	Y
BD-39	676.37	
BD-1	733.00	
TD-14b	785.28	
BD-35	**797.79**	
TD-9b	756.16	
BD-16	754.66	
TD-5c	751.64	I
TD-10b	751.51	N
BD-26	722.66	A
BD-42	688.47	C
BD-36	736.71	T
BD-20	778.58	I
BD-9	747.37	V
BD-2	749.62	E
TD-15b	646.61	S
BD-8	735.30	
TD-12b	774.33	
BD-17	739.45	
PD-3	**807.87**	
BD-5	766.41	

Table 6. Total energy (E_{TOTAL}) and RMS deviation values found for the receptor pruned models with the largest ligands, PD-3 and BD-35.

Receptor pruned models with the ligand PD-3	E_{TOTAL}[a] (kcal/mol)	RMS fit[b] (Å)
8 Å radii	−2213.20	1.94
10 Å radii	−5868.48	1.13
12 Å radii	−16587.19	1.27
Receptor pruned models with the ligand BD-35	**E_{TOTAL} (kcal/mol)**	**RMS fit (Å)**
8 Å radii	−2478.56	2.40
10 Å radii	−6299.63	1.09
12 Å radii	−16759.79	1.18

[a] Total energy, including solvation energy. [b] RMS deviation of receptor pruned compare to the entire FabI.

energy of bound receptor (E_R) equal to 10235.24 kcal/mol. The intramolecular energy was calculated including the solvation energy. The same kind of energy contributions were obtained for the lowest energy complex of FabI with BD-35/NAD adduct bound; the energy values are the following: 2390.47 kcal/mol (E_{TOTAL}), −61270.20 kcal/mol (E_{inter}), −234.09 kcal/mol (E_L), and 10227.00 kcal/mol (E_R) (data not presented in Table 7).

A comparison of ligand-receptor interaction energy of each receptor model reveals that the pruned receptor model of 12 Å radii is the most favorable for the two largest ligands PD-3 and BD-35 (see Table 7). Furthermore, when 20 ps MD simulations at 310K (nonbonded cutoff value of 12 Å) were performed for each of the pruned enzyme-largest ligands models the results are the same, indicating the pruned receptor model of 12 Å radii as the most favorable in terms of ligand-receptor interaction energy and RMS atomic positions value. This size of receptor model can be taken in all MD simulations as a compromise between reliability and computational efficiency to perform a *RD* 4D-QSAR analysis.

Stability of the receptor structure was optimal when the heavy mass constraint was assigned to all main chain atoms of the entire receptor pruned model. This constraint was used in all simulations.

4 Discussion

The receptor pruned model of 12 Å is the most energetically favorable and also maintains the conformational integrity of the composite parent crystal structure, according the total energy and RMS deviation values, respectively (Tables 6–7). The RMS fit value is smaller than 1.5 Å for the complexes containing the two largest ligands bound, PD-3/NAD and BD-35/NAD. The docking of those largest ligands in the active site demonstrated that all diazaborine derivatives can fit into and satisfy the 12 Å cutoff for the pruned receptor model.

Baldock and co-workers [3] reported the analysis of the diazaborine binding sites and they verified that the thieno- and benzo-diazaborine compounds bind in closely related manner, adjacent to the nicotinamide ring of the cofactor, in a pocket formed by the side chains of Tyr146, Tyr156, Met159, Ile200, Phe203, Leu100, Lys163, and the main chain peptide between Gly93 and Ala95. The substitutions

Table 7. Energy contributions and RMS deviation values found for the receptor pruned models with the largest ligands, PD-3 and BD-35, using a nonbonded cutoff value of 12 Å in MD calculations.

Receptor pruned models with the ligand PD-3	E_{TOTAL}[a] (kcal/mol)	E_{inter}[b] (kcal/mol)	E_L[c] (kcal/mol)	E_R[d] (kcal/mol)	RMS fit[e] (Å)
8 Å radii	−3933.42	−4644.76	−160.62	1165.08	1.96
10 Å radii	−8413.85	−9998.92	−160.07	2236.43	1.13
12 Å radii	−16587.19	−18734.71	−114.98	3556.50	1.27
Receptor pruned models with the ligand BD-35	**E_{TOTAL} (kcal/mol)**	**E_{inter} (kcal/mol)**	**E_L (kcal/mol)**	**E_R (kcal/mol)**	**RMS fit (Å)**
8 Å radii	−4480.87	−5260.20	−222.04	1139.30	2.17
10 Å radii	−8512.78	−9890.14	−217.31	2188.70	1.21
12 Å radii	−16759.79	−19024.68	−202.96	3496.12	1.18

[a] Total energy, including solvation energy. [b] Ligand-receptor intermolecular interaction energy. [c] Intramolecular energy, including solvation energy, of bound ligand. [d] Intramolecular energy, including solvation energy, of bound receptor. [e] RMS deviation of receptor pruned models compare to the entire FabI.

on organosulfonyl side chain seem to be relevant to the biological activity. The amino acid residues which could be involved in binding interactions are Gly93, Ala95, and Leu100 when a benzo-diazaborine (BD-1) is bound to FabI. However, when the ligand bound is a thieno-diazaborine (TD-18b) the amino acid residues which could be participated in binding interactions are Met159, Ile200, Gly93, and Phe94.

The integrity of Gly93 is crucial to maintain the inhibitory activity of diazaborines against FabI. A single mutation in *E. coli* ENR as Gly93Ser leads to diazaborine resistance [7, 29]. Additional interactions include hydrogen bonds between the boron hydroxyl and the phenolic hydroxyl of Tyr156 and between a nitrogen atom in the boron-containing ring and an ordered solvent molecule [3]. In this study, all scale-down receptor models presented the important amino acid residues in ligand-receptor binding interactions as part of their final structure. Thus, those primary interactions were considered in MD simulations to generate the energy contributions and respective sampling conformation of the ligand-receptor complexes.

The criteria for constraining atom movement possibly will be ligand-receptor dependent. The use of large fictitious masses is virtually the same as using Cartesian constraints. The heavy atomic masses were assigned to all backbone atoms of the reduced-size receptor models providing a convenient way to balance MD simulations motions in the pruned protein model that are similar to those of the complete parent protein model. Consequently, the obtained results are only relevant if the system retains a geometry "close" to that observed in the experimentally determined crystal state, during the MD procedures.

Here, the pruning was a preprocessing operation to scale down the enzyme FabI to a manageable size structure containing the main amino acid residues of the binding site before undertaking the actual 4D-QSAR formalism to a set of 51 diazaborine derivatives (Tables 1–3), our next work. The perspectives include the structure-based design of new antituberculosis agents regarding the identity in total amino acid sequence (28%) [6, 30] and the structural similarity in the active site (40%) [6, 30] shared by the ENRs from *E. coli* (FabI) and *M. tuberculosis* (InhA).

Acknowledgements

K. F. M. P. is grateful to the CNPq for scholarship support, to the FAPESP for financial support and to the Chem21 Group, Inc. for providing the license of MOLSIM 3.2 program used in this study.

References

[1] M. A.Grassberger, F. Turnowsky, J. Hildebrandt, *J. Med. Chem.* **1984**, *27*, 947–953.
[2] C. Baldock, J. B. Rafferty, S. E. Sedelnikova, P. J. Baker, A. R. Stuitje, A. R. Slabas, T. R. Hawkes, D. W. Rice, *Science* **1996**, *274*, 2107–2110.
[3] C. Baldock, G. J. de Boer, J. B. Rafferty, A. R. Stuitje, D. W. Rice, *Biochem. Pharmacol.* **1998**, *55*, 1541–1549.
[4] H. Bergler, S. Fuchsbichler, G. Högenauer, F. Turnowsky, *Eur. J. Biochem.* **1996**, *242*, 689–694.
[5] M. J. Stewart, S. Parikh, G. Xiao, P. J. Tonge, C. Kisker, *J. Mol. Biol.* **1999**, *290*, 859–865.
[6] D. A. Rozwarski, C. Vilchèze, M. Sugantino, R. Bittman, J. C. Sacchettini, *J. Biol. Chem.* **1999**, *274*, 15582–15589.
[7] M. M. Kater, G. M. Koningstein, H. J.J. Nijkamp, A. R. Stuitje, *Plant Mol. Biol.* **1994**, *25*, 771–790.
[8] K. Magnuson, S. Jackowski, C. O. Rock, J. E. Cronan Jr., *Microbiol. Rev.* **1993**, *57*, 522–542.
[9] C. E. Barry III, R. E. Lee, K. Mdluli, A. E. Sampson, B. G. Schroeder, R. A. Slayden, Y. Yuan, *Prog. Lipid Res.* **1998**, *37*, 143–179.
[10] A. D. McCarthy, D. G. Hardie, *Trends Biochem. Sci.* **1984**, *9*, 60–63.
[11] K. F. M. Pasqualoto, E. I. Ferreira, *Curr. Drug Targets* **2001**, *2*, 427–437.
[12] K. F. M. Pasqualoto, E. I. Ferreira, O. A. Santos-Filho, A. J. Hopfinger, *J. Med. Chem.* **2004**, *47*, 3755–3764.
[13] J. S. Tokarski, A. J. Hopfinger, *J. Chem. Inf. Comput. Sci.* **1997**, *37*, 779–791.
[14] A. J. Hopfinger, S. Wang, J. S. Tokarski, B. Jin, M. G. Albuquerque, P. J. Madhav, C. Duraiswami, *J. Am. Chem. Soc.* **1997**, *119*, 10509–10524.
[15] M. G. Albuquerque, A. J. Hopfinger, E. J. Barreiro, R. B. Alencastro, *J. Chem. Inf. Comput. Sci.* **1998**, *38*, 925–938.
[16] M. Ravi, A. J. Hopfinger, R. E. Hormann, L. Dinan, *J. Chem. Inf. Comput. Sci.* **2001**, *41*, 1587–1604.
[17] O. A. Santos-Filho, A. J. Hopfinger, *Quant. Struct.-Act. Relat.* **2002**, *43*, 324–336.
[18] X. Hong, A. J. Hopfinger, *J. Chem. Inf. Comput. Sci.* **2003**, *43*, 324–336.
[19] D. Pan, Y. Tseng, A. J. Hopfinger, *J. Chem. Inf. Comput. Sci.* **2003**, *43*, 1591–1607.
[20] D. Pan, L. Jianzhong, C. Senese, A. J. Hopfinger, Y. Tseng, *J. Med. Chem.* **2004**, *47*, 3075–3088.
[21] F. C. Berstein, T. F. Koetzle, G. J. B. Williams, E. F. Meyer, M. D. Brice, J. R. Rodgers, O. Kennard, T. Shimanouchi, M. Tasumi, *J. Mol. Biol.* **1977**, *112*, 535–542.
[22] S. J. Weiner, P. A. Kollman, D. T. Nguyen, *J. Comput. Chem.* **1986**, *7*, 230–252.
[23] HyperChem Program Release 6.03 for Windows, 2000, Hybercube, Inc., Gainesville, FL.
[24] D. Doherty, MOLSIM: Molecular Mechanics and Dynamics Simulation Software. User's Guide, version 3.2, 1997, The Chem21 Group, Inc., Lake Forest, IL.
[25] M. J.S. Dewar, E. G. Zoebisch, E. F. Healy, J. J.P. Stewart, *J. Am. Chem. Soc.* **1985**, *107*, 3902–3909.
[26] N. Bodor, Z. Gabanyi, C. K. Wong, *J. Am. Chem. Soc.* **1989**, *111*, 3783–3786.
[27] A. Gavezzotti, *J. Am. Chem. Soc*. **1983**, *105*, 5220–5225.
[28] A. J. Hopfinger. In: Conformational Properties of Macromolecules, Academic Press, New York, 1973, pp. 71.
[29] F. Turnowsky, K. Fuchs, C. Jeschek, G. Hogenauer, *J.Bacteriol.* **1989**, *171*, 6555–6565.
[30] A. Dessen, A. Quémard, J. S. Blanchard, W. R. Jacobs, J. C. Sacchettini, *Science* **1995**, *267*, 1638–1641.

